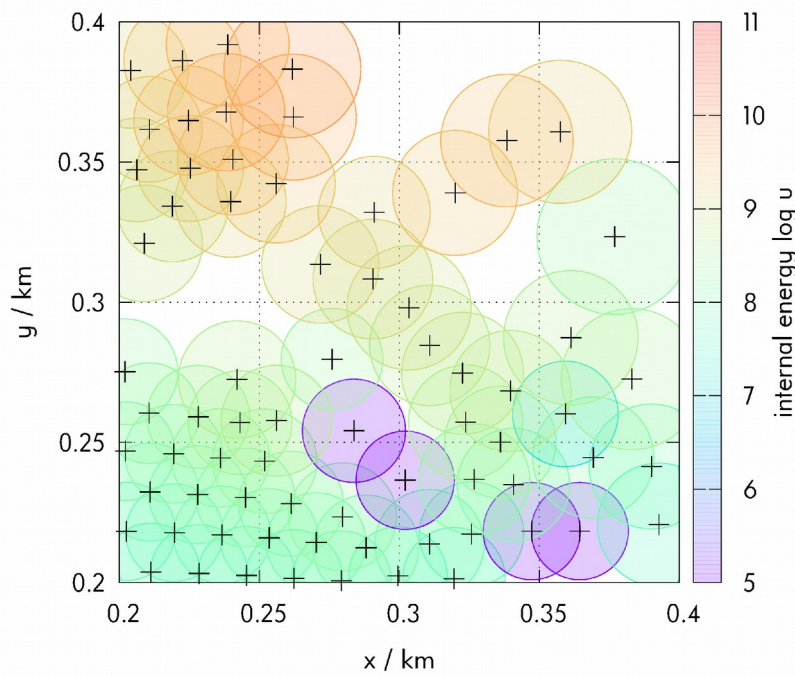


Hydrodynamics and SPH method

1. our problem
2. SPH approximation
3. initial conditions
4. two phases
5. observations!
6. other problems



Our problem is:

$$\frac{d\rho}{dt} = -\rho \nabla \cdot \mathbf{v},$$

$$\frac{d\mathbf{v}}{dt} = -\frac{1}{\rho} \nabla P - \nabla \Phi + \frac{1}{\rho} \nabla \cdot \mathbf{S},$$

$$\frac{dU}{dt} = -P \nabla \cdot \mathbf{v} + \mathbf{S} \cdot \frac{1}{2} [\nabla \mathbf{v} + (\nabla \mathbf{v})^T],$$

$$\nabla^2 \Phi = 4\pi G \rho,$$

$$P = \begin{cases} A\left(\frac{\rho}{\rho_0} - 1\right) + B\left(\frac{\rho}{\rho_0} - 1\right)^2 + a\rho U + \frac{b\rho U}{\frac{U}{U_0} \frac{\rho_0^2}{\rho^2} + 1} & \text{pro } U < U_{\text{iv}}, \\ a\rho U + \left[\frac{b\rho U}{\frac{U}{U_0} \frac{\rho_0^2}{\rho^2} + 1} + A\left(\frac{\rho}{\rho_0} - 1\right) e^{-\beta\left(\frac{\rho_0}{\rho} - 1\right)} \right] e^{-\alpha\left(\frac{\rho_0}{\rho} - 1\right)} & \text{pro } U > U_{\text{cv}}, \end{cases}$$

$$\frac{d\mathbf{S}}{dt} = 2\mu_1 \frac{1}{2} [\nabla \mathbf{v} + (\nabla \mathbf{v})^T] + \left(\mu_2 - \frac{2}{3}\mu_1\right) \nabla \cdot \mathbf{v} \mathbf{I}.$$

Aha!

Basic equations

basic
equations

$$\frac{d\rho}{dt} = -\rho \nabla \cdot \mathbf{v}, \quad \text{eq. of continuity}$$

lagrangian
formulation

$$\frac{d\mathbf{v}}{dt} = -\frac{1}{\rho} \nabla P - \nabla \Phi + \frac{1}{\rho} \nabla \cdot \mathbf{S}, \quad \text{Navier-Stokes}$$

$$\frac{dU}{dt} = -P \nabla \cdot \mathbf{v} + \mathbf{S} \cdot \frac{1}{2} [\nabla \mathbf{v} + (\nabla \mathbf{v})^T], \quad \text{1st law of thermodynamics}$$

$$\nabla^2 \Phi = 4\pi G \rho, \quad \text{Poisson}$$

eq. of state
(Tillotson 1962)

$$P = \begin{cases} A\left(\frac{\rho}{\rho_0} - 1\right) + B\left(\frac{\rho}{\rho_0} - 1\right)^2 + a\rho U + \frac{b\rho U}{\frac{U}{U_0} \frac{\rho_0^2}{\rho^2} + 1} & \text{pro } U < U_{\text{iv}}, \\ a\rho U + \left[\frac{b\rho U}{\frac{U}{U_0} \frac{\rho_0^2}{\rho^2} + 1} + A\left(\frac{\rho}{\rho_0} - 1\right) e^{-\beta\left(\frac{\rho_0}{\rho} - 1\right)} \right] e^{-\alpha\left(\frac{\rho_0}{\rho} - 1\right)} & \text{pro } U > U_{\text{cv}}, \end{cases}$$

$$\frac{d\mathbf{S}}{dt} = 2\mu_1 \frac{1}{2} [\nabla \mathbf{v} + (\nabla \mathbf{v})^T] + \left(\mu_2 - \frac{2}{3}\mu_1\right) \nabla \cdot \mathbf{v} \mathbf{I}. \quad \text{constitutive relation (for solids)}$$

Additional equations

- yielding criterion (von Mises 1913)

$$\mathbf{S} = f \mathbf{S}, \quad f = \min \left[\frac{Y^2}{3J_2}, 1 \right], \quad J_2 = S^{\alpha\beta} S^{\alpha\beta},$$

- flaws distribution (Weibull 1938) → cracks, damage D

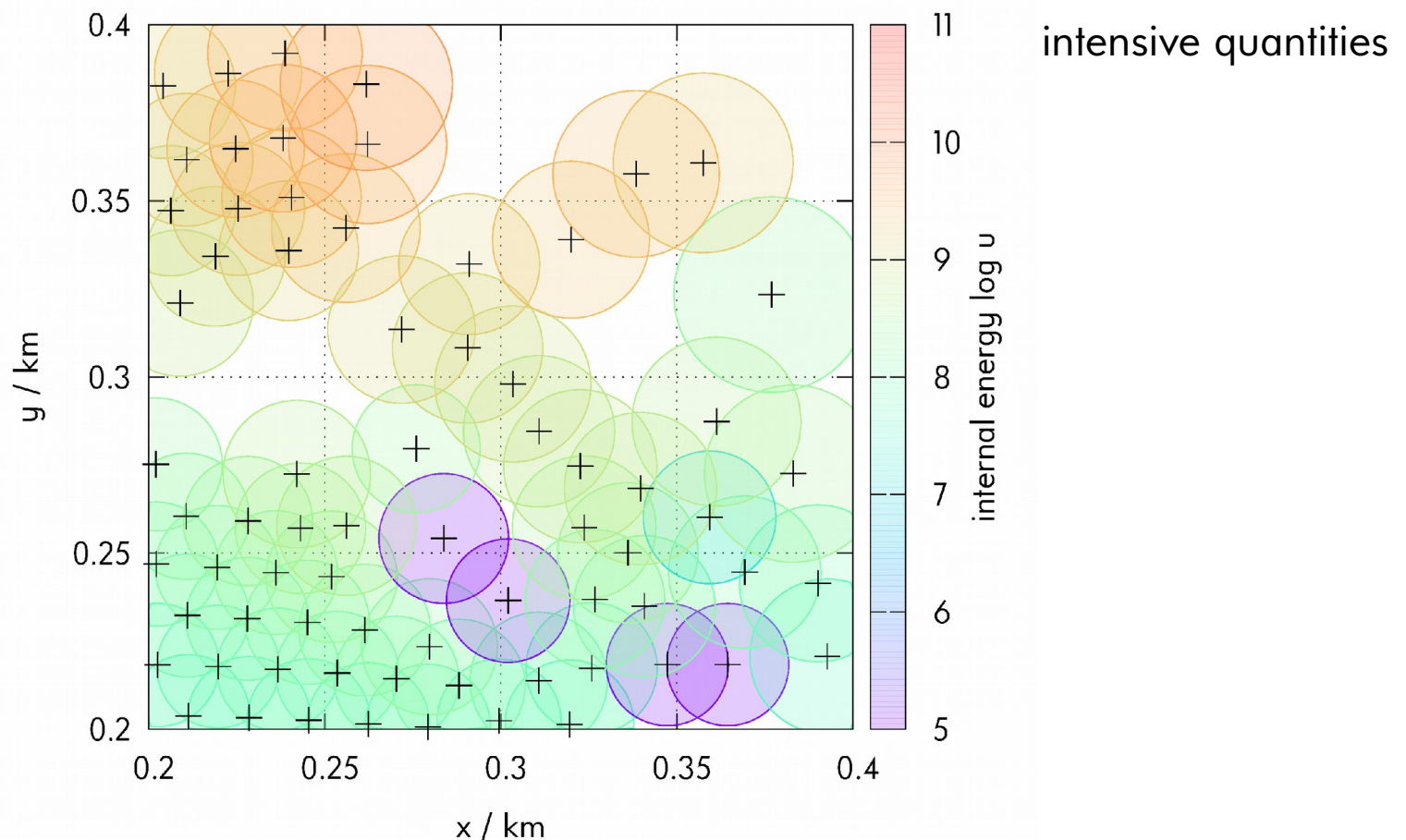
$$\sigma_{\alpha\beta} = \begin{cases} -P\delta_{\alpha\beta} + (1-D)S_{\alpha\beta} & \text{pro } P \geq 0, \\ -(1-D)P\delta_{\alpha\beta} + (1-D)S_{\alpha\beta} & \text{pro } P < 0. \end{cases}$$

$$\frac{dD^{\frac{1}{3}}}{dt} = \left[\left(\frac{c_g}{R_s} \right)^3 + \left(\frac{m+3}{3} \alpha^{\frac{1}{3}} \epsilon^{\frac{m}{3}} \right)^3 \right]^{\frac{1}{3}}, \quad \text{Grady \& Kipp (1980)}$$

smoothed particle →

SPH approximation

- continuum → a finite set of extended particles (“vehicles”),
cf. Cossins (2010), Price (2012)



SPH formulation

- an integral representation of functions & discretisation

$$\mathbf{v}(\mathbf{r}) = \int_{\Omega} \mathbf{v}(\mathbf{r}') \delta(|\mathbf{r} - \mathbf{r}'|, h) d\Omega \doteq \int_{\Omega} \mathbf{v}(\mathbf{r}') W(|\mathbf{r} - \mathbf{r}'|, h) d\Omega,$$

$$\begin{aligned}\nabla \cdot \mathbf{v}(\mathbf{r}) &= \int_{\Omega} [\nabla_{r'} \cdot \mathbf{v}(\mathbf{r}')] W(|\mathbf{r} - \mathbf{r}'|, h) d\Omega = \\ &= \int_{\Omega} \nabla_{r'} \cdot [\mathbf{v}(\mathbf{r}') W(|\mathbf{r} - \mathbf{r}'|, h)] d\Omega - \int_{\Omega} \mathbf{v}(\mathbf{r}') \cdot \nabla_{r'} W(|\mathbf{r} - \mathbf{r}'|, h) d\Omega = \\ &\quad = 0 \text{ na hranici} \\ &= \int_{\partial\Omega} \mathbf{v}(\mathbf{r}') \overbrace{W(|\mathbf{r} - \mathbf{r}'|, h)}^{\text{d}\vec{\Gamma}} d\vec{\Gamma} - \dots = \\ &= - \int_{\Omega} \mathbf{v}(\mathbf{r}') \cdot \nabla_{r'} W(|\mathbf{r} - \mathbf{r}'|, h) d\Omega = \int_{\Omega} \mathbf{v}(\mathbf{r}') \cdot \nabla_r W(|\mathbf{r} - \mathbf{r}'|, h) d\Omega,\end{aligned}$$

$$\nabla \cdot \mathbf{v}_i \doteq \sum_{j=1}^{N_{\text{okolo}}} \mathbf{v}_j \cdot \nabla W(|\mathbf{r}_i - \mathbf{r}_j|, h) \frac{m_j}{\rho_j},$$

SPH formulation (cont.)

- spatial derivatives → summations over nearest *neighbours*
- discretization in time (Euler or predictor/corrector)

$$\rho_i^{n+1} = \rho_i^n - \Delta t \rho_i^n \sum_j \mathbf{v}_j^n \cdot \nabla W_{ij}(h) \frac{m_j}{\rho_j^n},$$

$$\mathbf{v}_i^{n+1} = \mathbf{v}_i^n - \frac{\Delta t}{\rho_i^n} \sum_j P_j^n \nabla W_{ij}(h) \frac{m_j}{\rho_j^n} + \frac{\Delta t}{\rho_i^n} \sum_j \mathbf{s}_j^n \cdot \nabla W_{ij}(h) \frac{m_j}{\rho_j^n},$$

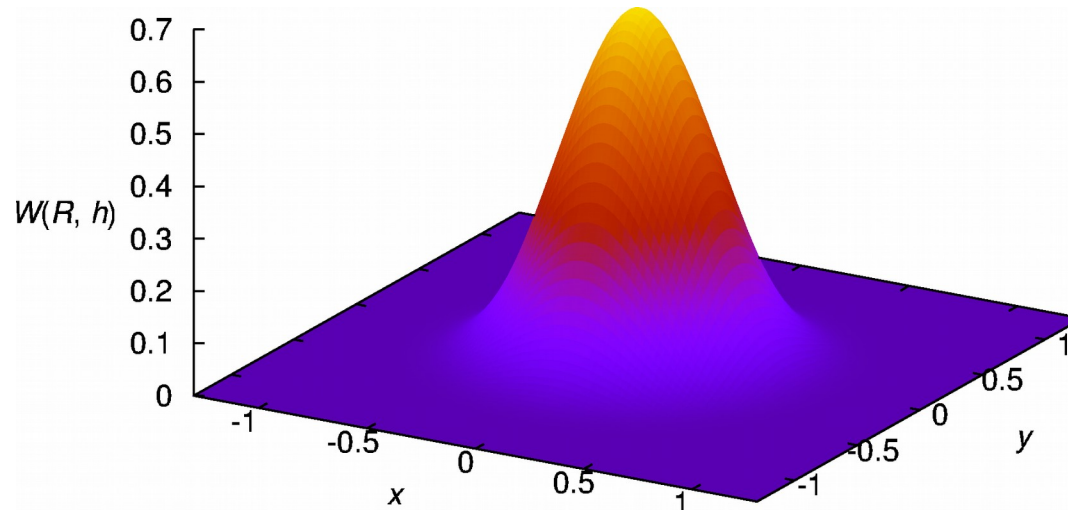
$$U_i^{n+1} = U_i^n - \Delta t P_i^n \sum_j \mathbf{v}_j^n \cdot \nabla W_{ij}(h) \frac{m_j}{\rho_j^n} +$$

$$+ \sum_{\alpha=1}^3 \sum_{\beta=1}^3 S_{\alpha\beta}^n \frac{1}{2} \sum_j \left[v_{\beta j}^n \frac{\partial}{\partial x_\alpha} W_{ij}(h) + v_{\alpha j}^n \frac{\partial}{\partial x_\beta} W_{ij}(h) \frac{m_j}{\rho_j^n} \right].$$

Smoothing Kernel

- suitable function: normal, compact, $\lim_{h \rightarrow 0} W(h) = \delta$, positive, decreasing, symmetric, smooth

$$W(R, h) = \frac{3}{2\pi h^3} \begin{cases} \frac{2}{3} - 4R^2 + 4R^3 & \text{pro } 0 \leq R < \frac{1}{2}, \\ \frac{4}{3} - 4R + 4R^2 - \frac{4}{3}R^3 & \text{pro } \frac{1}{2} \leq R < 1, \\ 0 & \text{pro } R \geq 1. \end{cases}$$



Obr. 2 — Kubický spline $W(R, h)$ dle rovnice (15).

Initial & boundary conditions

- initial: $r \sim 2$ spheres, diameters $D_{\text{target}}, d_{\text{project}}$, homogeneous,
 $\mathbf{v} = \text{const.}$, impact angle φ_{imp} , no rotation
- no boundary (free surfaces)
- material parameters: $\rho_0, A, B, U_0, a, b, \alpha, \beta, U_{\text{iv}}, U_{\text{cv}}, \mu, \underline{\gamma}, U_{\text{melt}}, k, m \leftarrow$ a lot of...
- numerical integration: adaptive timestep Δt , Courant number $C = 1$, timespan $t_2 \simeq 3$ days

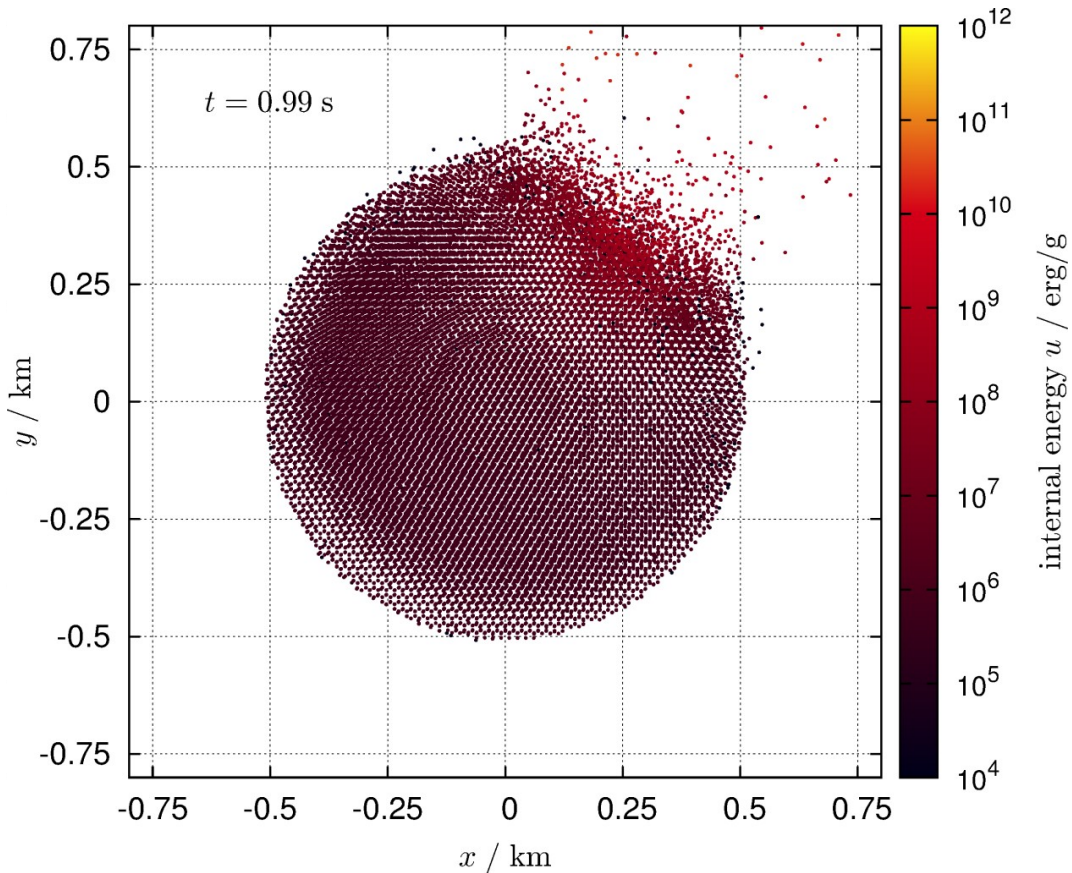
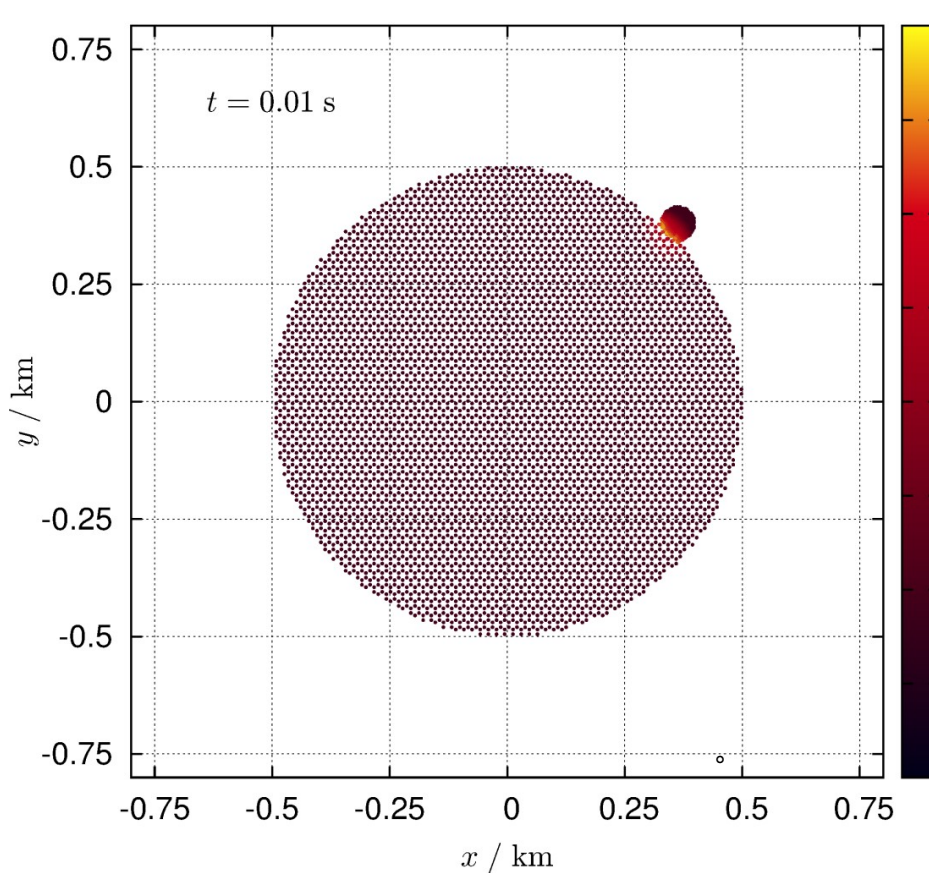
gravity free →

don't worry,
be happy...

Fragmentation phase

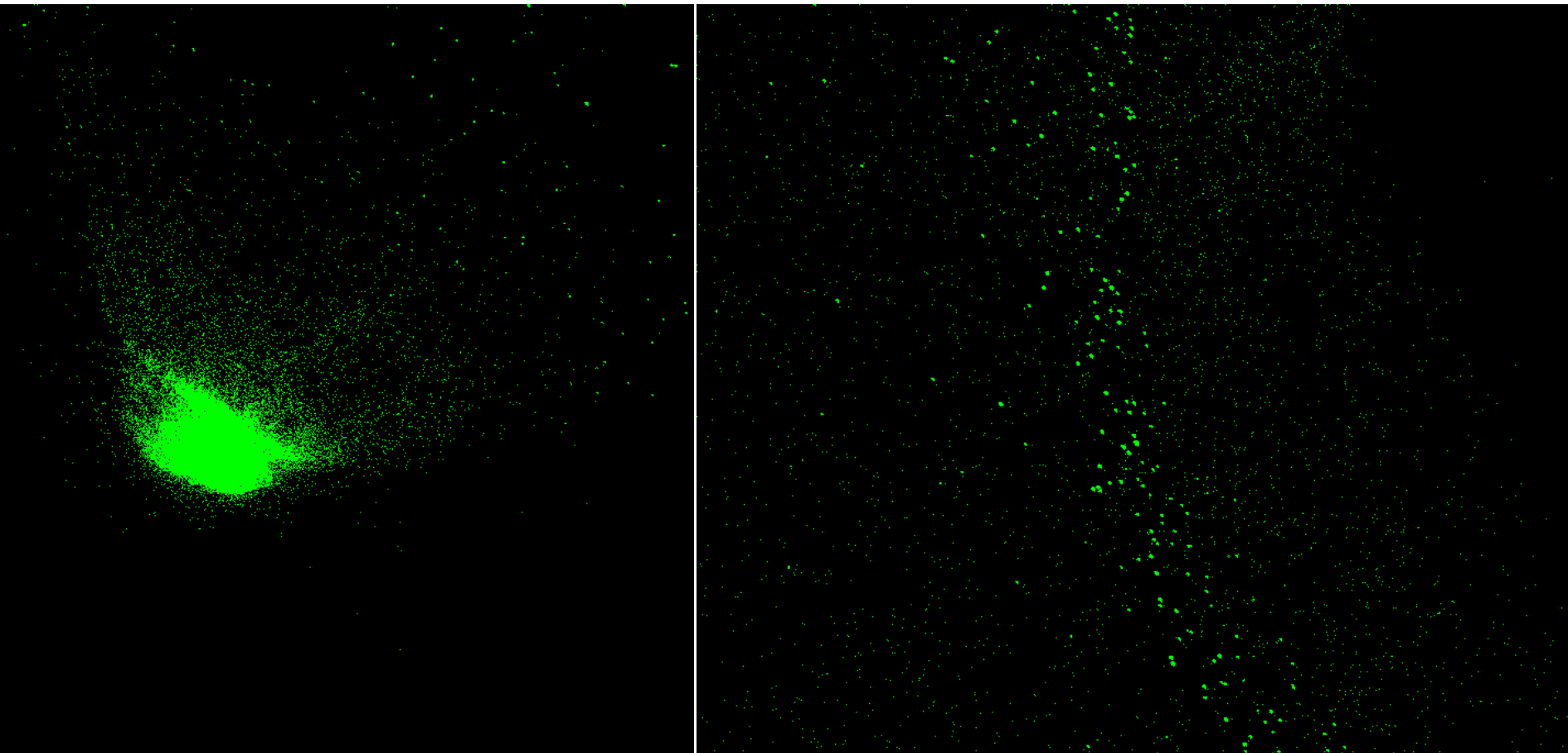
- hydrodynamic approach, SPH5 code (Benz & Asphaug 1994)

$$D = 1 \text{ km}, d = 0.074 \text{ km}, v_{\text{imp}} = 5 \text{ km/s}, \varphi_{\text{imp}} = 45^\circ, Q/Q^*_D = 9.837$$



gravity *only* → **Reaccumulation phase**

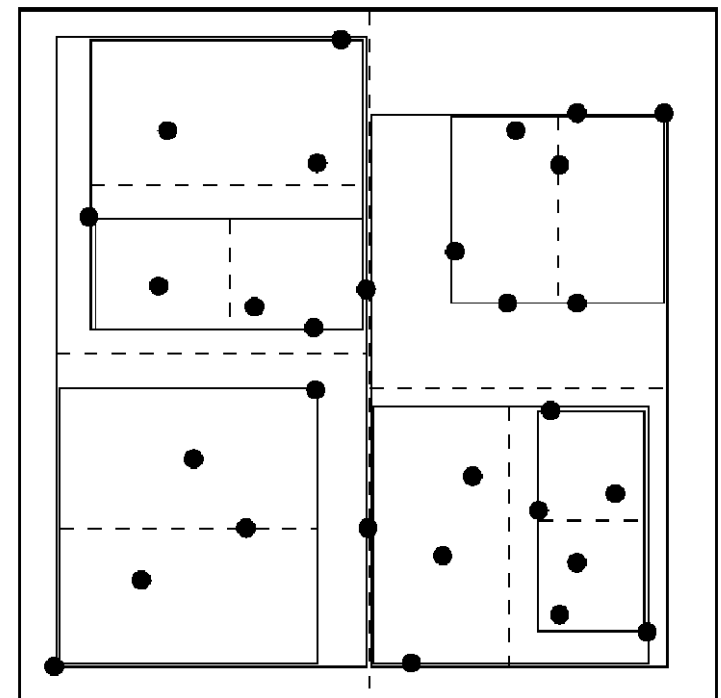
- N -body approach, k -d tree, only spheres, perfect merging, pkdgrav code (Richardson et al. 2009)



i.e. *three-dimensional* →

k-d tree

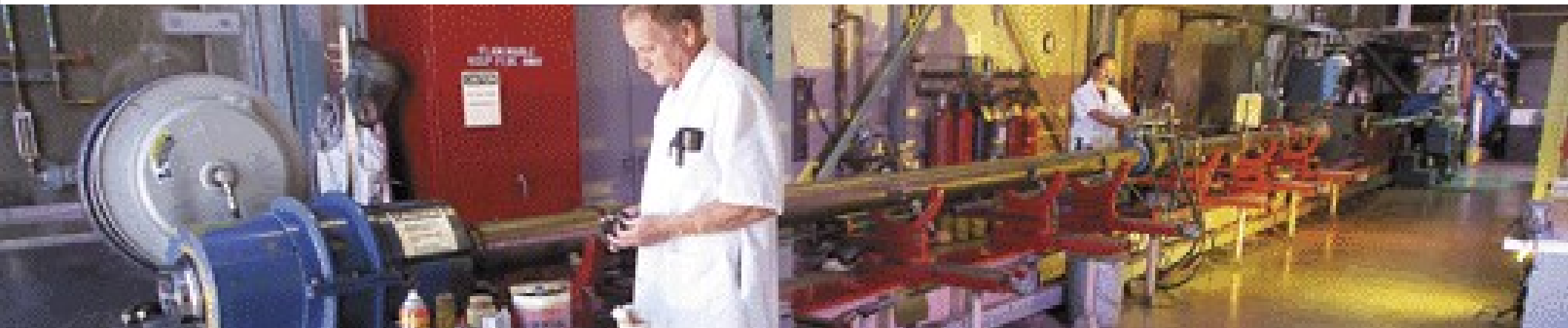
- split a group of points according to x, y, z, x, \dots coordinates
- gravity approximation, nearest-neighbour search, ...
- 4th-order multipole expansion for particle↔cell interactions
- opening angle $\varphi \simeq 0.5$, large vs small
- alternatives: linked-list (in SPH5)



Uncertainties related to SPH

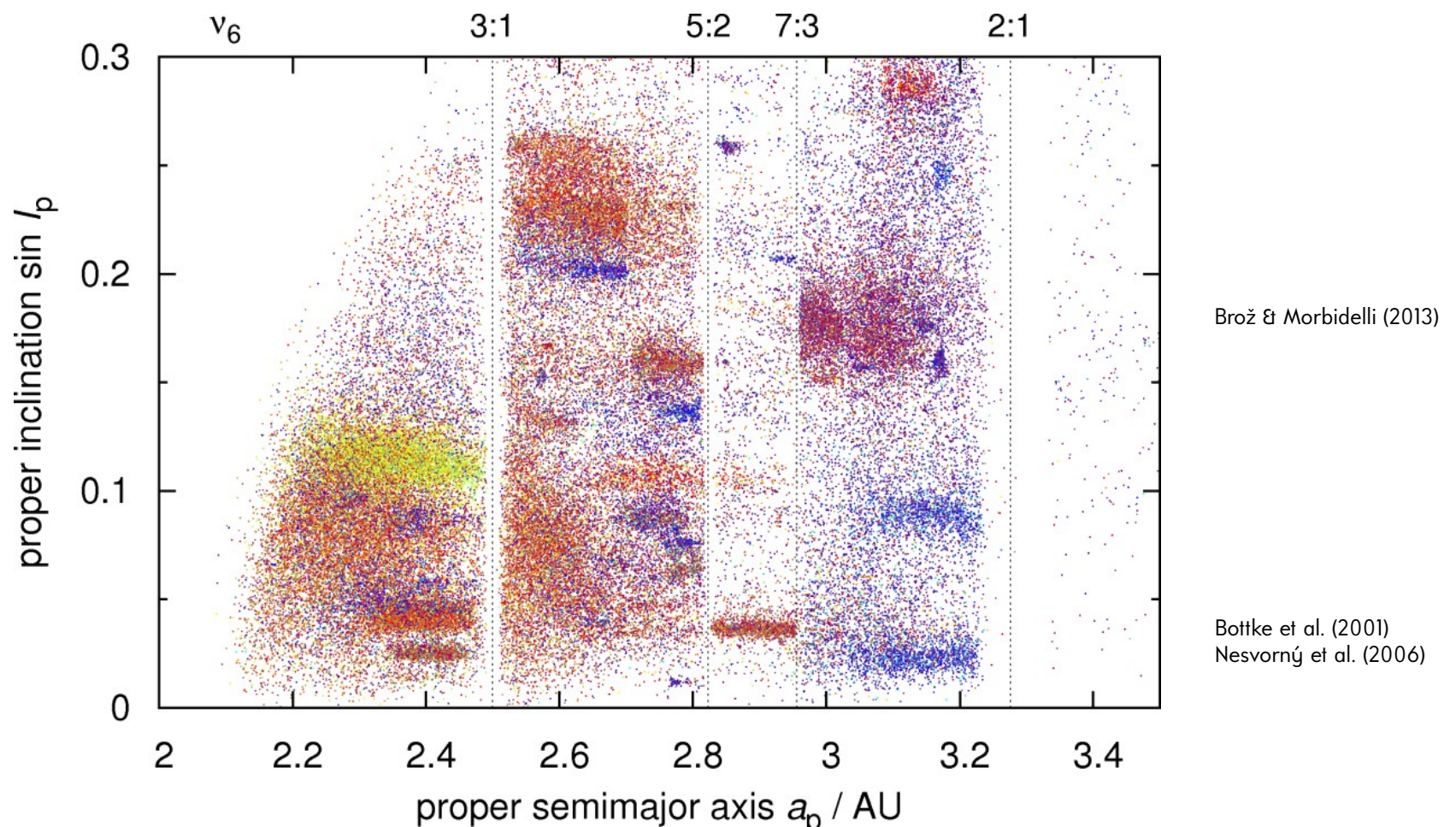
- material parameters (moduli, flaws)
- state equation, phase transitions (e.g. ANEOS, SESAME)
- chemical reactions (!) in gaseous phase
- *total* damage → dust clouds?
- bouncing and friction in reaccumulation phase
- no information on fragment shapes and rotation yet
- laboratory experiments, e.g. for icy projectiles

Livermore ↓



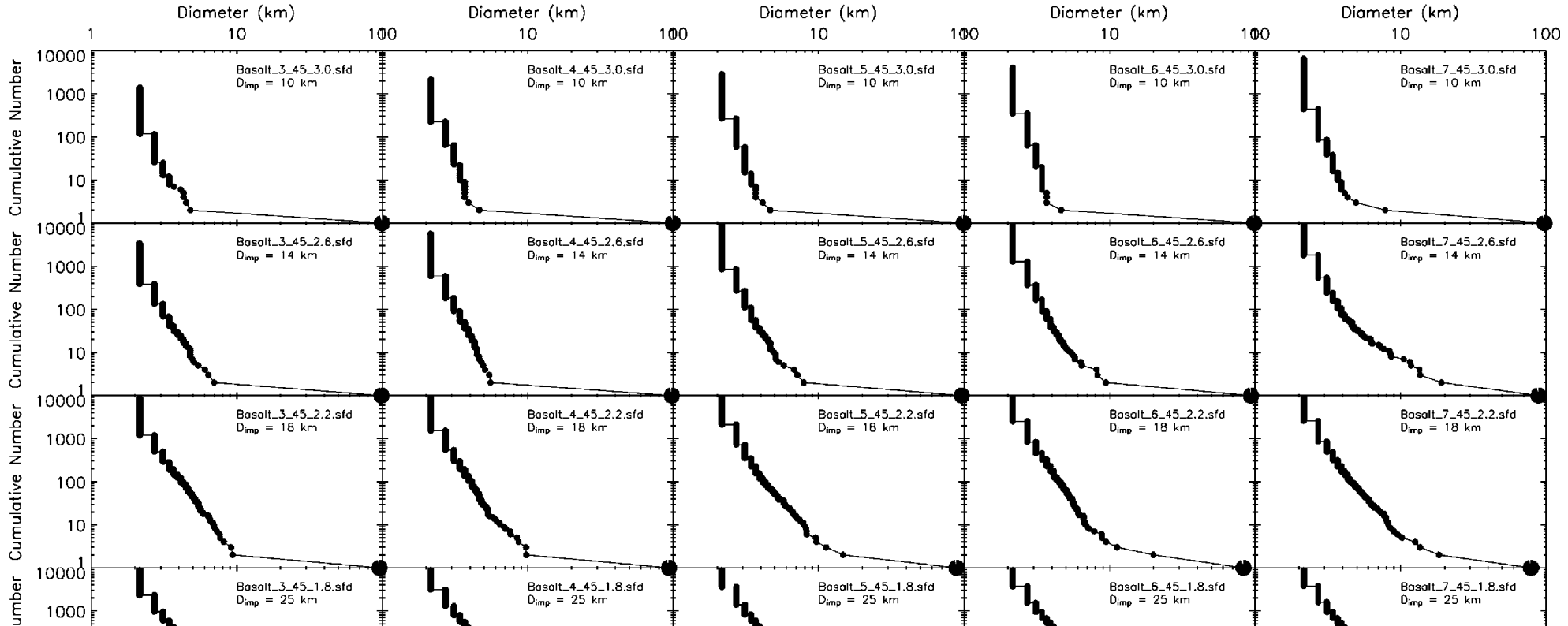
Observed asteroid families \leftarrow finally!

- e.g. Nesvorný et al. (2015), Brož et al. (2013), ...



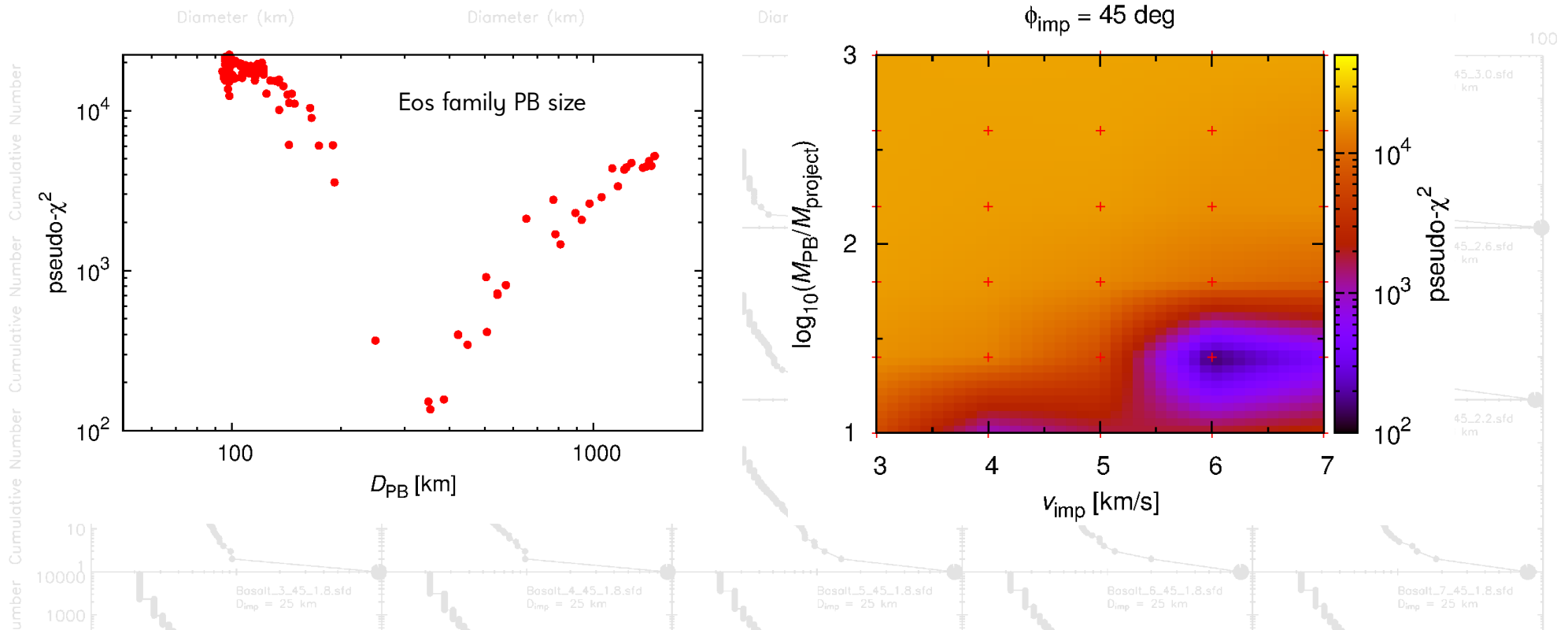
Parent-body size(s)

- a simplified scaling (Durda et al. 2007), cf. Tanga et al. (1999)
- uncertainties: multiple fits have low χ^2 , interlopers
- systematics: number & distribution of SPH particles



Parent-body size(s)

- a simplified scaling (Durda et al. 2007), cf. Tanga et al. (1999)
- uncertainties: multiple fits have low χ^2 , interlopers
- systematics: number & distribution of SPH particles



Monte-Carlo collisional models

(e.g. Boulder code, Morbidelli et al. 2009)

- Monte-Carlo approach
- number of disruptions
- parametric relations (SPH)
- largest remnant
- largest fragment
- SFD slope of fragments
- dynamical decay

pseudo-random-number generator
for rare collisions within one time step

specific energy $Q = \frac{1}{2} m_i v^2 / M_{\text{tot}}$

Q_D^* ... scaling law

focussing

$$n_{ij} = p_i(t) f_g \frac{(D_i + d_j)^2}{4} n_i n_j \Delta t$$

$$M_{\text{LR}} = \left[-\frac{1}{2} \left(\frac{Q}{Q_D^*} - 1 \right) + \frac{1}{2} \right] M_{\text{tot}} \quad \text{for } Q < Q_D^*$$

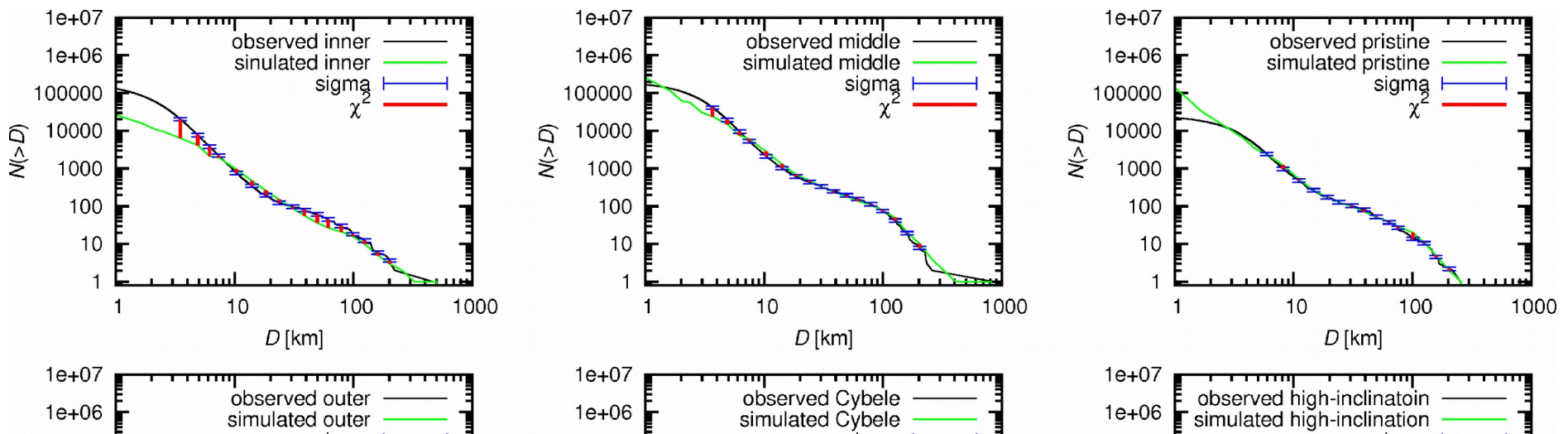
$$M_{\text{LR}} = \left[-0.35 \left(\frac{Q}{Q_D^*} - 1 \right) + \frac{1}{2} \right] M_{\text{tot}} \quad \text{for } Q > Q_D^*$$

$$M_{\text{LF}} = 8 \times 10^{-3} \left[\frac{Q}{Q_D^*} \exp \left(- \left(\frac{Q}{4Q_D^*} \right)^2 \right) \right] M_{\text{tot}}$$

$$q = -10 + 7 \left(\frac{Q}{Q_D^*} \right)^{0.4} \exp \left(- \frac{Q}{7Q_D^*} \right)$$

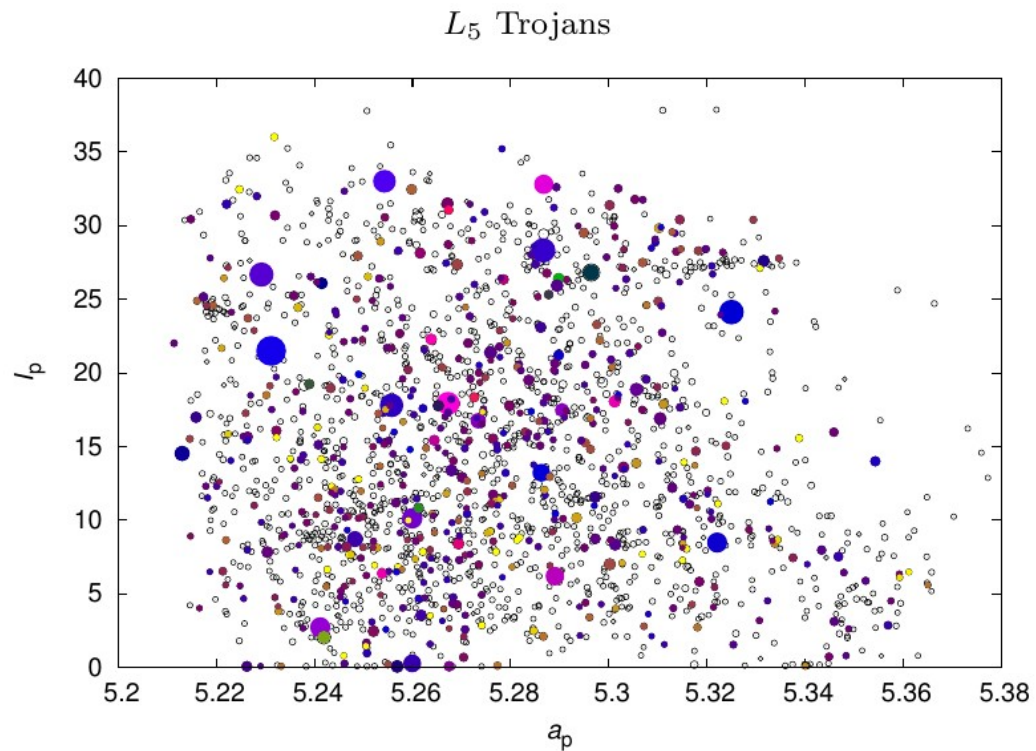
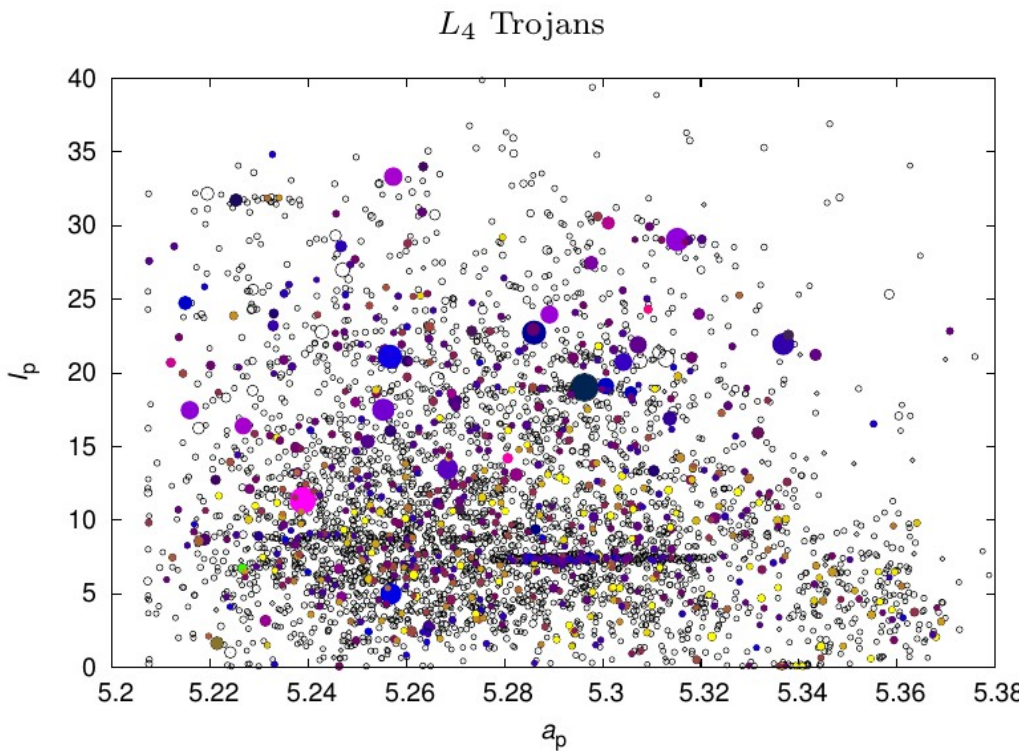
Monte-Carlo collisional models

- for rubble-piles see Cibulková et al. (2014)
- for $D_{\text{PB}} = 1 \text{ km}$ see Ševeček et al. (in prep.)
- still some problems with energy conservation: initial decompression wave, double precision, increased artificial viscosity (to resolve shock-wave)



Jupiter Trojans

- 1:1 mean-motion resonance with Jupiter, Lagrange points
- resonant elements ← approximate integrals of motion



Jupiter Trojans

- hierarchical clustering (Zappalà et al. 1995), “randombox”
- families: Eurybates, Hektor, 1996 RJ, Arkesilaos & Ennomos, 2001 UV₂₀₉

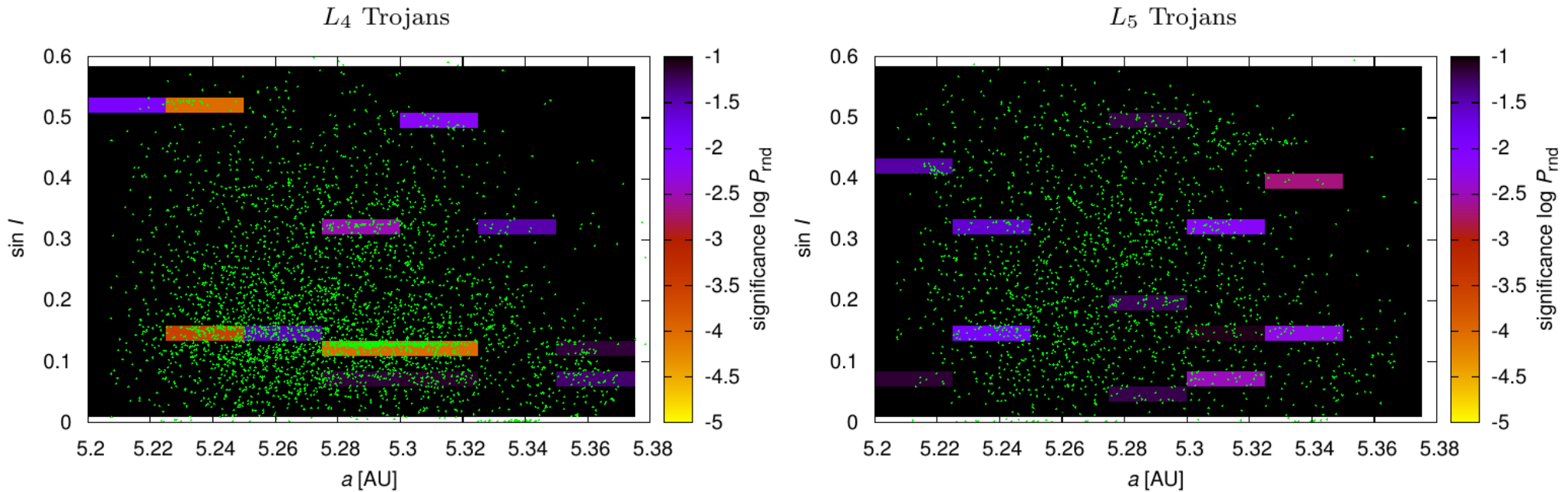


Figure 4. The statistical significance p expressed as colour on the logarithmic scale for observed asteroids in the proper semimajor axis vs proper inclination plane (a_p , $\sin I_p$) (i.e. the same data as in Figure 1). L_4 Trojans are on the left, L_5 Trojans on the right. We computed the values of p for 7 times 18 boxes using our “randombox” method. The range in proper eccentricity is 0.00 to 0.20. Statistically significant groups appear as orange boxes and they correspond to the families reported in Table 1.

Jupiter Trojans

- Hektor family, an exceptional (primitive) D taxonomical type

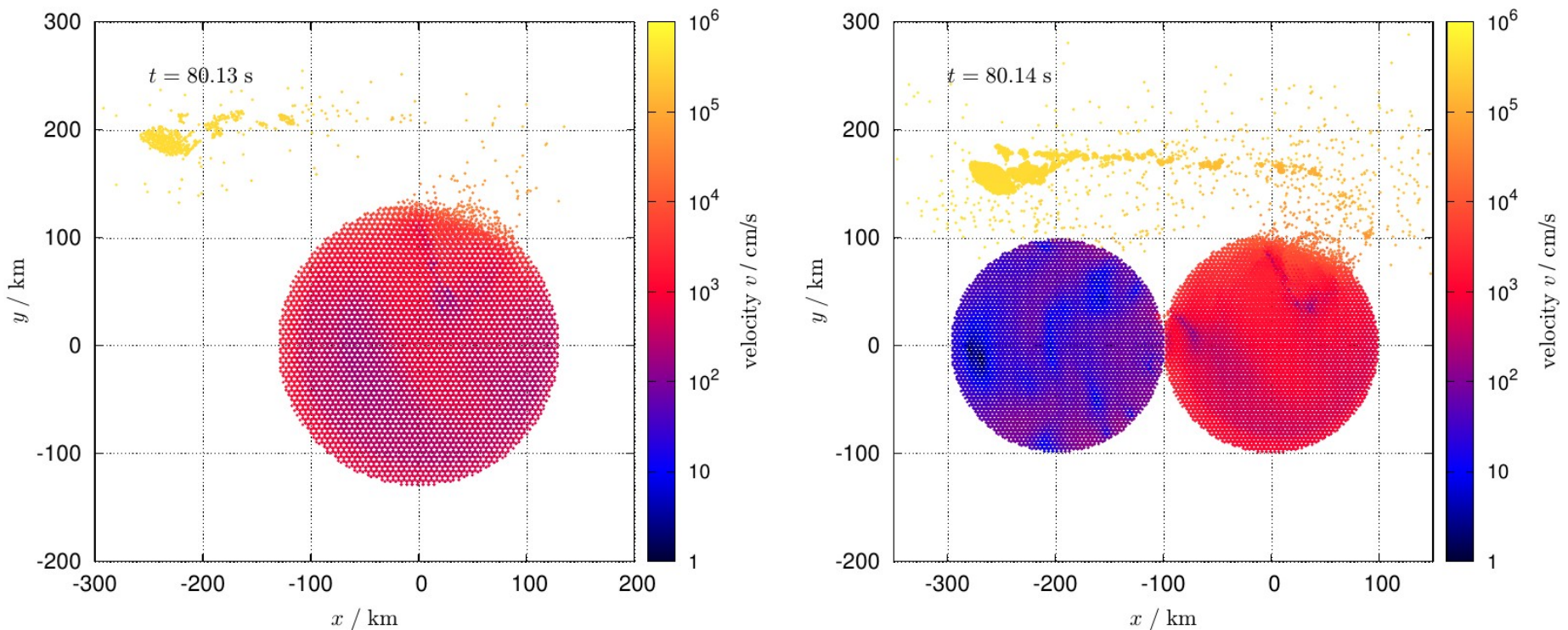


Figure 14. A comparison of SPH simulations of a disruption of a single body (basalt) with diameter $D_{\text{target}} = 250 \text{ km}$, by an impactor with the diameter $D_{\text{imp}} = 48 \text{ km}$ (silicate ice) (left) and a disruption of a bilobe basalt target, with $D_{\text{target}} = 198 \text{ km}$ for each sphere, by an impactor with $D_{\text{imp}} = 46 \text{ km}$ (silicate ice) (right). Time elapsed is $t = 80.1 \text{ s}$ in both cases. There are notable physical differences between the two simulations, especially in the propagation of the shock wave, which is reflected from free surfaces, the number of secondary impacts, or the fragmentation (damage) of the target. Nevertheless, the amount of ejected material and the resulting size-frequency distributions do not differ that much (cf. Figure 11).

Jupiter Trojans

- differences of SFD rather minor, thought
- parameter space of impact geometries much larger!

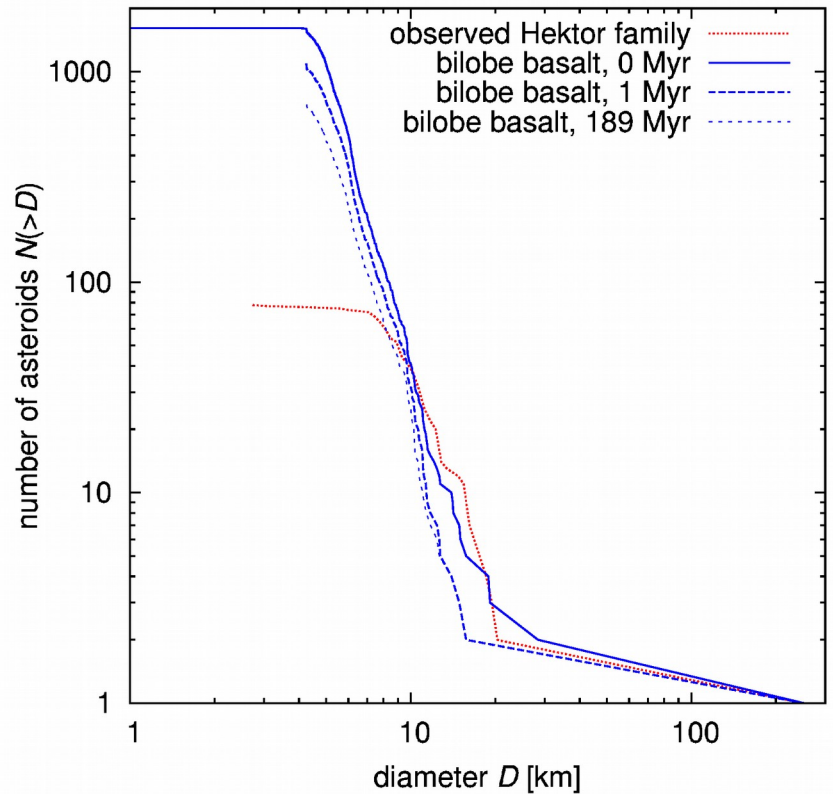
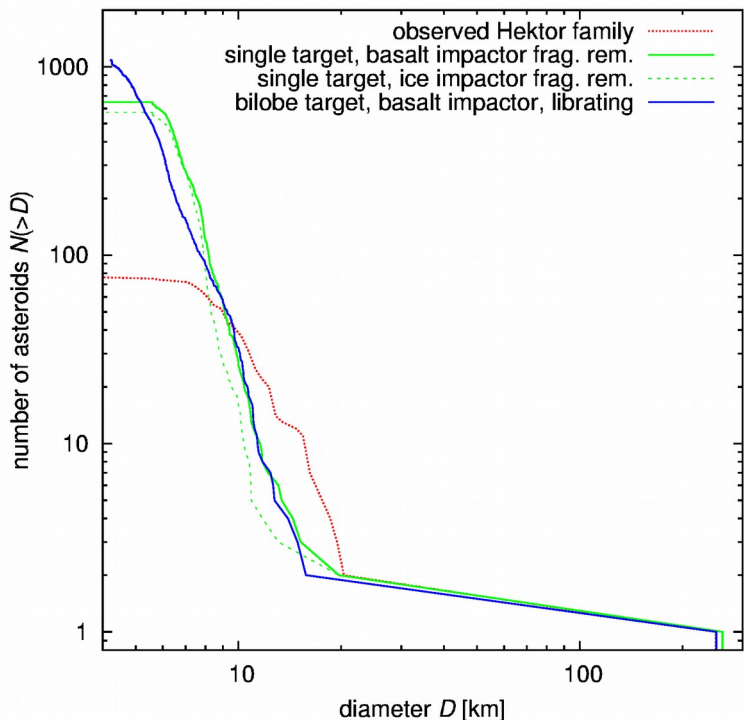
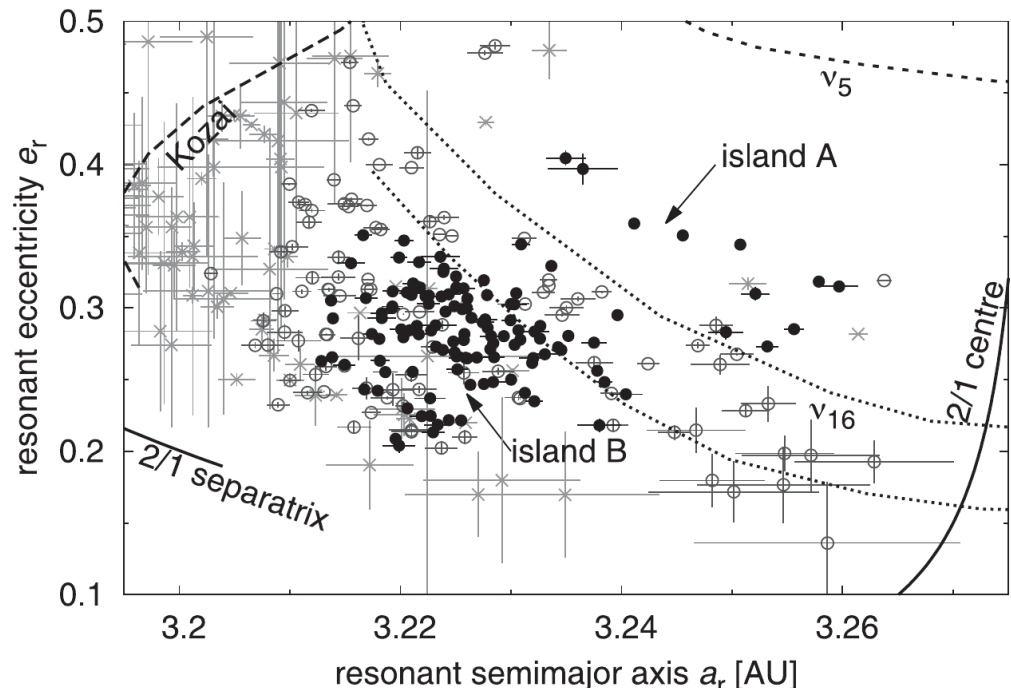
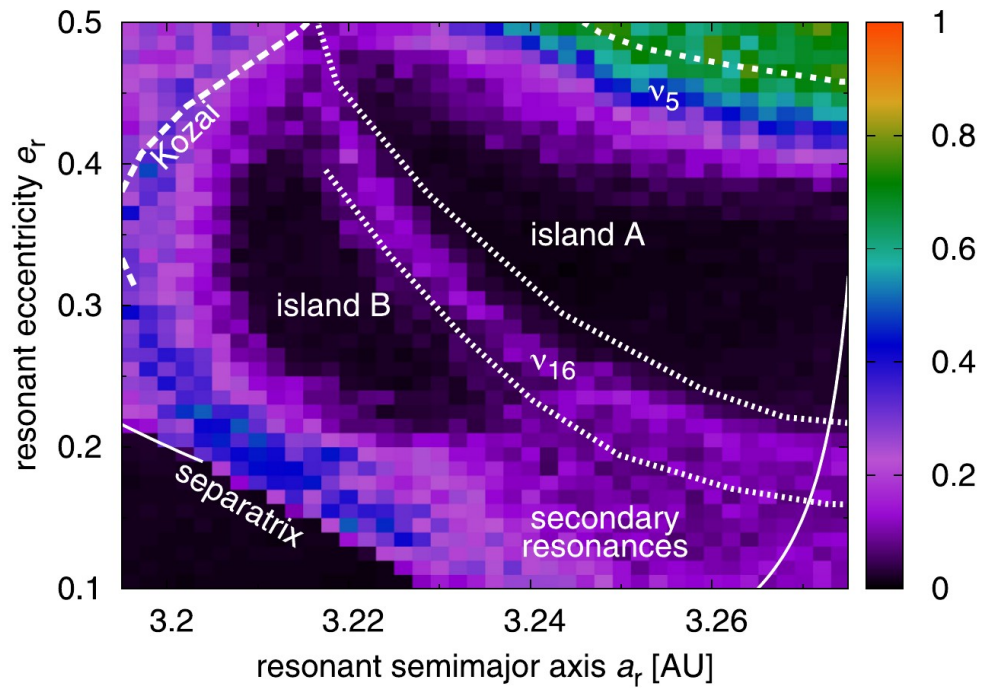


Figure 12. A simulation of evolution of the SFD of a synthetic Hektor family due to a ballistic transport and chaotic diffusion. One can see here a rapid change of SFD within the first 1 Myr after the breakup as the fragments of the impactor leaved the libration zone in our impact geometry. This ballistic transport resulted in a reduction of the number of particularly larger bodies in our case. Further evolution due to the chaotic diffusion seems to cause the reduction of mostly smaller bodies.

2:1 resonance with Jupiter

- unstable asteroids \leftarrow delivered by YE (Brož et al. 2005) easy...
- stable asteroids (Chrenko et al. 2015)
- two stable islands A & B, $\tau \approx 1$ Gyr, ratio 1:10



2:1 resonance with Jupiter

- fifth planet & jumping-Jupiter scenario (Nesvorný & Morbidelli 2012)

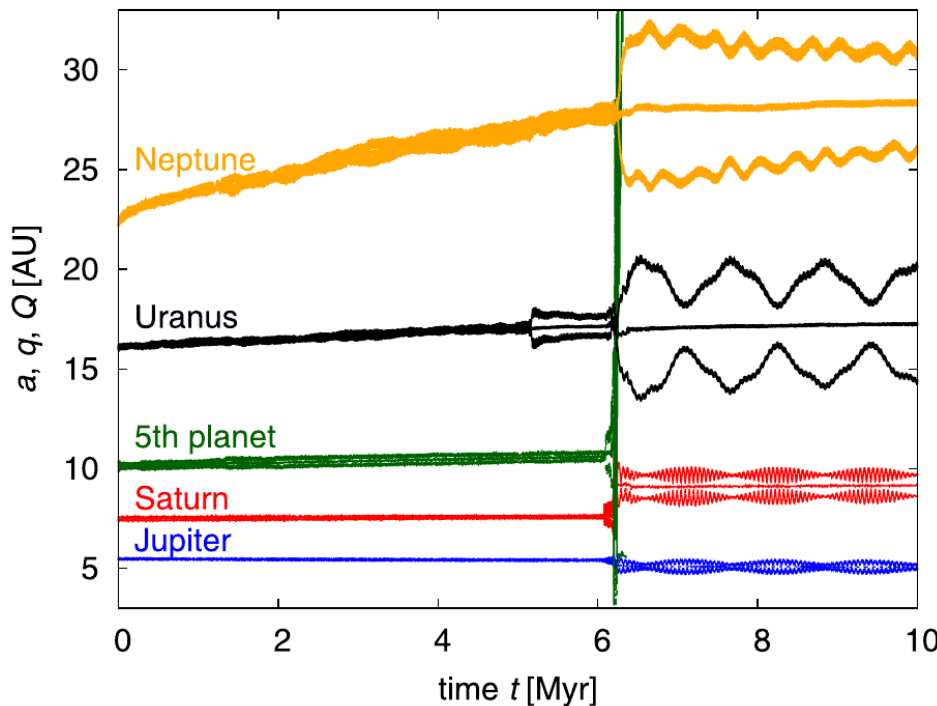
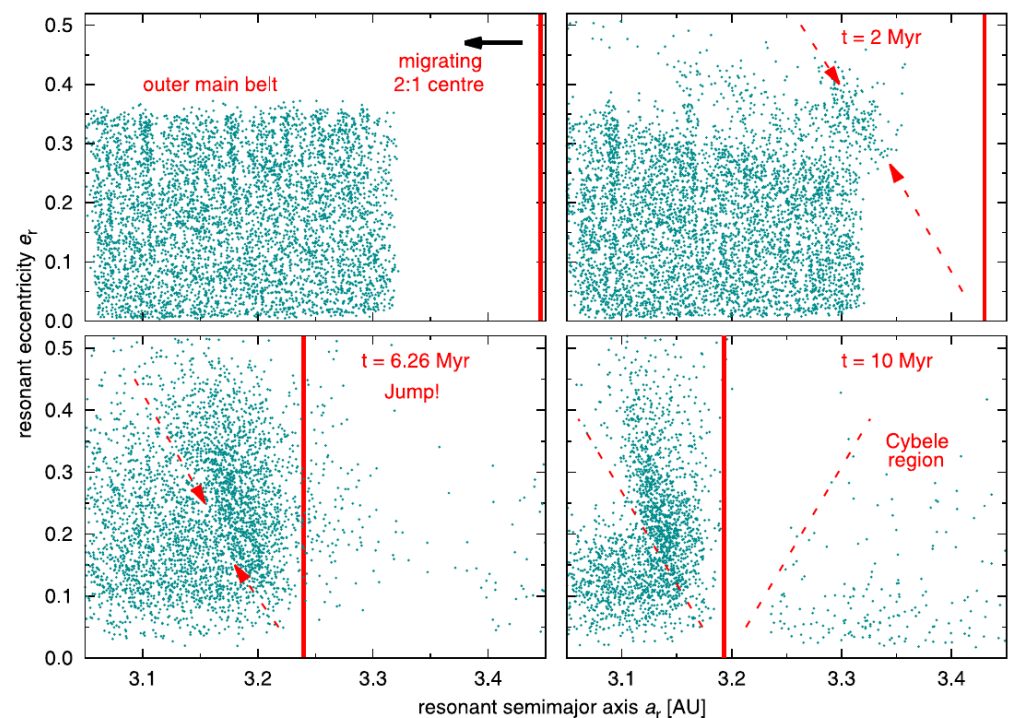


Figure 7. Orbital evolution of giant planets in the fifth giant planet scenario, adopted from Nesvorný & Morbidelli (2012), during the jumping-Jupiter instability, as it was reproduced by our modified integrator. We plot the time t versus the semimajor axis a , the pericentre q and the apocentre Q . Each evolutionary track is labelled with the name of the corresponding giant planet.



simulation of the resonant capture from the outer main belt in the fifth giant planet scenario (Nesvorný & Morbidelli 2012). We plot the test particles in the resonant semimajor axis a_r versus resonant eccentricity e_r plane. The vertical line indicates an approximate location of the 2:1 resonance. Jupiter migrates inwards together with Jupiter. The integration time is shown in three of the panels ($t = 0, 2, 6.26$ and 10 Myr) and corresponds to the panels in Fig. 7. The dashed arrows and lines indicate an approximate extent of the libration zone in the case of the migrating and stable resonance. From top to bottom and left to right, the plots show: the initial conditions, the relaxed population of test particles prior to jump, the starting of the jumping-Jupiter instability and the final state. Note that all test particles are depicted in terms of resonant elements for simplicity (even the non-resonant ones).

2:1 resonance with Jupiter

- problem: steep SFD $\gamma = -4.5$, usually due to recent collision
- *but* no observable family
- solution: a significant change of SFD due to spatial gradient

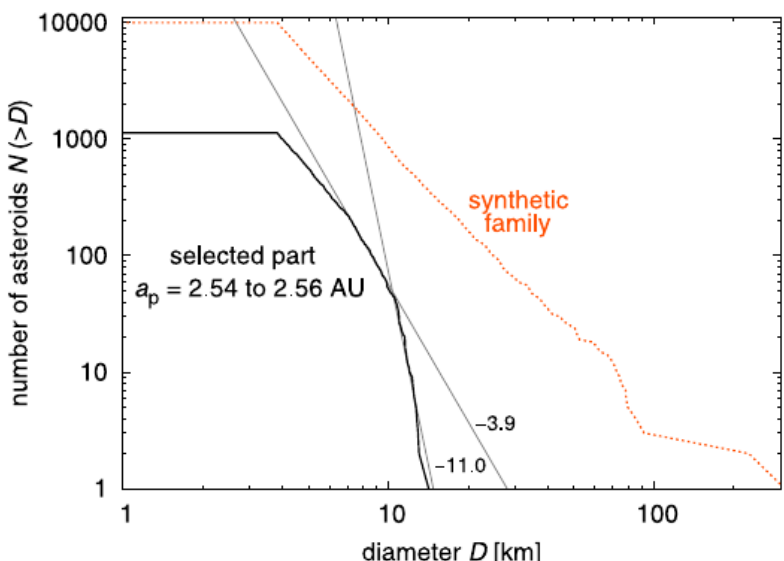
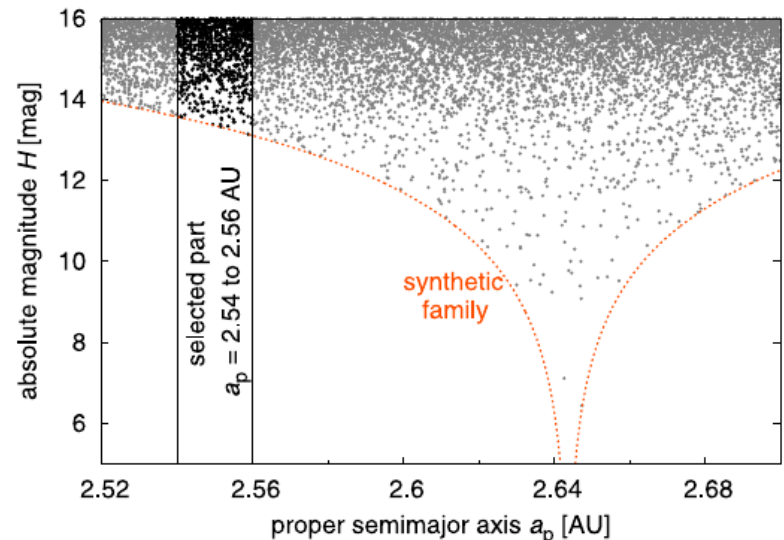


Figure 16. Dependence of the absolute magnitude H on the proper semimajor axis a_p and the size distribution of the synthetic family.

Finite element method

- Ševeček et al. (2015), notation Langtangen (2003):

$$\mathcal{L} \equiv \rho C \partial_t - \nabla \cdot K \nabla, \quad \mathcal{L}(u) = 0. \quad K \partial_n u + \epsilon \sigma u^4 = (1 - A) \Phi \vec{s} \cdot \vec{n},$$



$$u \doteq \hat{u} = \sum_{j=1}^M u_j N_j,$$

$$\int_{\Omega} \mathcal{L}(\hat{u}) N_i d\Omega = 0.$$

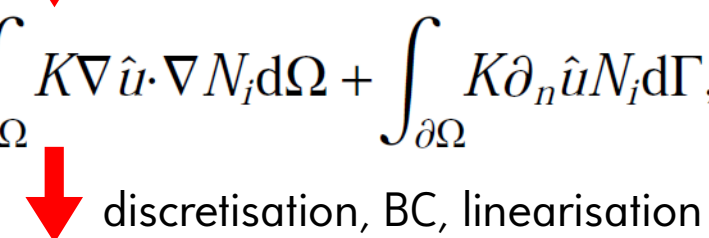
weak formulation
Galerkin method



$$\int_{\Omega} \rho C \partial_t \hat{u} N_i d\Omega - \int_{\Omega} \nabla \cdot (K \nabla \hat{u}) N_i d\Omega = 0.$$



$$\int_{\Omega} \nabla \cdot (K \nabla \hat{u}) N_i d\Omega = - \int_{\Omega} K \nabla \hat{u} \cdot \nabla N_i d\Omega + \int_{\partial\Omega} K \partial_n \hat{u} N_i d\Gamma,$$

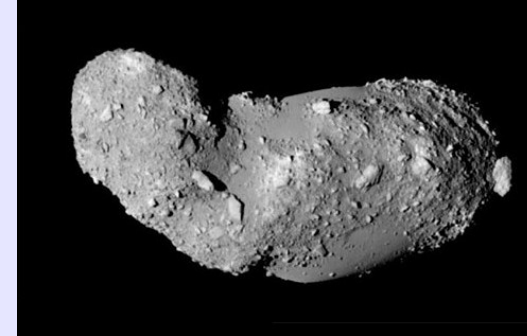


$$\int_{\Omega} \frac{\rho C}{\Delta t} \hat{u}^n N_i d\Omega - \int_{\Omega} \frac{\rho C}{\Delta t} \hat{u}^{n-1} N_i d\Omega + \int_{\Omega} K \nabla \hat{u} \cdot \nabla N_i d\Omega +$$

$$+ \int_{\partial\Omega} \epsilon \sigma (\hat{u}^{n-1})^3 \hat{u}^n N_i d\Gamma - \int_{\partial\Omega} (1 - A) \Phi \vec{s} \cdot \vec{n} N_i d\Gamma = 0.$$

Individual

Boulders on Itokawa



- 3-dimensional heat diffusion (Golubov & Krugly 2012, Ševeček et al. 2015) → non-negligible YORP torques
- uncertainties: SFD of boulders, thermal parameters
- systematics: real shapes

cf. Lowry et al. (2014)

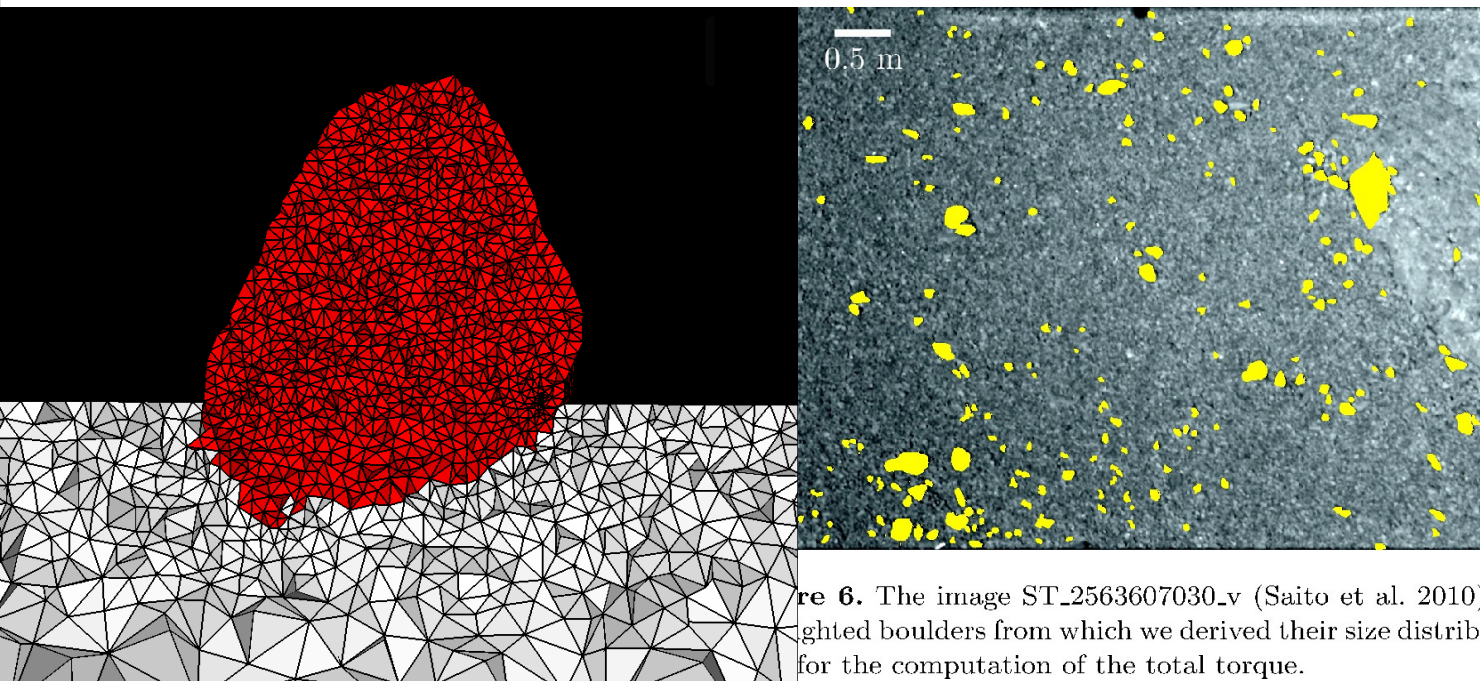
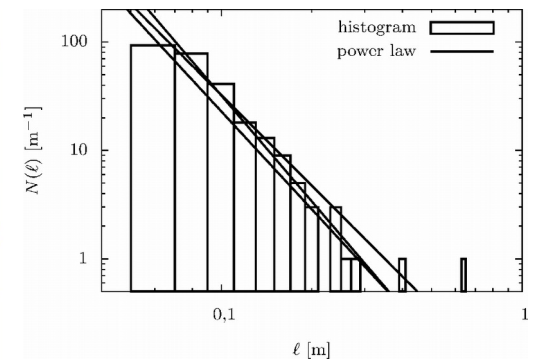


Figure 6. The image ST_2563607030_v (Saito et al. 2010) with highlighted boulders from which we derived their size distribution, for the computation of the total torque.



$d\omega/dt \sim 10^{-7} \text{ rad day}^{-2}$
for (25143) Itokawa

Other remaining problems:

- 3D heat diffusion in small irregular meteoroids
- planetesimals embedded in protoplanetary disks *versus* mean-motion resonances (Chrenko & Brož, in prep.)

